European Journal of Radiology Open 3 (2016) 60–66

Contents lists available at ScienceDirect

European Journal of Radiology Open

journal homepage: www.elsevier.com/locate/ejro

# Influence of the short-axis cine acquisition protocol on the cardiac function evaluation: A reproducibility study

Stephanie Marchesseau*, Jamie X.M. Ho, John J. Totman

*Clinical Imaging Research Centre, ASTAR-NUS, Singapore, Singapore*

ARTICLE INFO

*Article history:*
Received 16 November 2015
Received in revised form 16 March 2016
Accepted 18 March 2016
Available online 23 March 2016

*Keywords:*
Cine MRI
Short-axis acquisition
Reproducibility study
Right ventricle
Left ventricle

ABSTRACT

*Purpose:* To define the optimal cardiac short-axis cine acquisition protocol for the assessment of the left and rightventricular functions.
*Materials and methods:* 20 volunteers were recruited and breath-hold CINE images were acquired on a Siemens Prisma 3T MRI. Four short-axis acquisition planes were defined from the 4-chamber view. *AV Junctions*: short-axis slices parallel to the plane that cuts through the external right and left atrioventricular junctions. *Left AV Junctions*: short-axis slices parallel to the plane that cuts through both left atrioventricular junctions. *Septum*: short-axis slices perpendicular to the septum with one cutting through the septum junction. *LongAxis*: short-axis slices perpendicular to the long axis with one cutting through the septum junction. Intra and inter reproducibility was assessed using Bland-Altman coefficient of variation (CV) and Lin's concordance correlation coefficient (CCC). The influence of the protocol on the ejection fraction (EF) and stroke volume (SV) was quantified statistically using pair-wise CV and Pearson's correlation coefficient $R^2$.
*Results:* All protocols led to high reproducibility for the LV EF (mean intra CV = 3.83%, mean inter CV = 4.81%, lowest CV = 4.20% (AV junctions) and highest CV = 5.24% (Left AV Junctions)). Reproducibility of the RV measurements was lower (mean intra CV = 7.84%, mean inter CV = 9.17%). Septum protocol led to significantly lower variability compared to the other 3 protocols for RV EF (CV = 7.62% (Septum), CV = 8.42% (Long Axis), CV = 9.54% (Left AV Junctions) and CV = 11.08% (AV Junctions) with Lin's CCC varying from 0.4 (AV Junctions) to 0.69 (Septum) for inter-observer reproducibility). No differences in group average for clinical parameters was found for both LV and RV clinical measurements. However, patient-specific RV EF evaluation is dependent on the chosen protocol (CV = 9.95%, $R^2$ = 0.52).
*Conclusion:* Based on the results of the study cine mode short-axis acquisitions should be planned perpendicular to the septum in order to guarantee optimal RV and LV measurements.


## 1. Introduction

The diagnosis and follow up of cardiovascular diseases are very challenging. Choosing the appropriate test to perform as well as measuring accurately the desired quantities is of high importance to make reliable, relevant clinical decisions. Cardiovascular Magnetic Resonance (CMR) imaging has proven to give more reproducible and accurate evaluation of the left and right ventricular functions compared to other modalities [1–4], mainly due to its high temporal resolution combined with a high spatial resolution which allow to cover the entire heart and the entire cardiac cycle [5]. Analysing these images with accuracy is challenging and requires specific training [6]. In particular, reproducibility of the measurements for the right ventricle (RV) seems to be adequate only with long processing times (45 min) [7,8] not compatible with routine practice. Therefore, current clinical studies on RV function must include a large data sample [9] for the group differences to be significant. This reproducibility issue is mainly due to the choice of the basal slice to include in the segmentation, for the left ventricle (LV) and the RV [10], in spite of precise guidelines to perform this selection [11]. Consistency in the imaging protocols is essential to compare results over different studies and for multi-center trials. The standard CMR protocol for the assessment of the left and right ventricular function includes 3 long axis slices (2-chamber view, 3-chamber view and 4-chamber view) and 10–14 contiguous short-axis slices. Each of these slices is a 2-dimensional (2D) image over 20–25 time frames, in order to represent the full

* Corresponding author.
*E-mail addresses:* dnrsmlp@nus.edu.sg, Stephyyyyy@gmail.com (S. Marchesseau).

http://dx.doi.org/10.1016/j.ejro.2016.03.003

cardiac cycle. Although, axial plane assessment of RV function has been shown to be more robust [12], the standard protocol still consist of the short-axis slices in order to evaluate both ventricles without increasing scanning time, as described by the SCMR guidelines [13]. The orientation of the short-axis stack is ambiguous and variation in clinical protocols exists. Conventionally, the short-axis slice orientation is defined from the 4-chamber view at end-diastole. It then varies from being perpendicular to the septum [14], or perpendicular to the long axis (defined as the axis passing through the apex and the center of the mitral valve) as prescribed by the SCMR 2008 guidelines [13]. Another definition commonly used forces the first slice to be placed across the atrioventricular valve plane. For a specific evaluation of the RV function, an acquisition plane from the outflow tract to increase accuracy can also be defined [15]. In this study, since the accuracy of the segmentation cannot be assessed by comparison with a true value, the optimal acquisition protocol will be defined as the one leading to the most reproducible results. Intra and inter observer variability will be measured for several short-axis orientation protocols as well as the influence of these protocols on the clinical parameters. Therefore, this studies aims at defining the optimum imaging protocol alignment for simultaneous measurement of RV and LV function using short-axis cine CMR imaging.

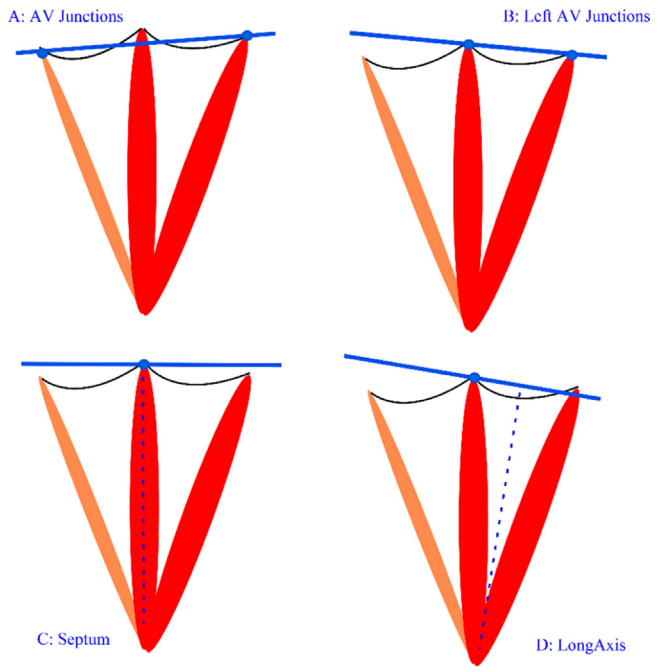


**Fig. 1.** Definition of the 4 protocols. (A) *AV Junctions*: short-axis slices parallel to the plane that cuts through the right and the left atrioventricular junctions. (B) *Left AV Junctions*: short-axis slices parallel to the plane that cuts through the left atrioventricular junction. (C) *Septum*: short-axis slices perpendicular to the septum with one cutting through the septum junction. (D) *Long Axis:* short-axis slices perpendicular to the long axis with one cutting through the septum junction.

## 2. Methods

### 2.1. Study population

The study population consisted of 20 healthy volunteers without known cardiovascular diseases (mean age 33, range 22–69, mean weight 67.9 kg, range 46–120 kg, 10 males). Exclusion criteria were standard for MRI studies (no metallic device, no pregnant woman, claustrophobia). Ethical approval was obtained and all subjects gave written consent. The sample size was limited by the acquisition time of approximately 20 min more than one standard cine protocol. This protocol was therefore limited to healthy volunteers not undergoing other CMR imaging sequences [16].

### 2.2. CMR acquisition

The study was performed using a 3T MR system (MAGNETOM Prisma, Siemens, Erlangen, Germany) equipped with an anterior 18-element matrix coil and a posterior 32-element spine matrix coil. Images were obtained with ECG-gating and breath-holding. The scanning protocol was as follows: 1) Transverse True fast imaging with steady state precession (TrueFISP) single-shot sequence of the whole heart was performed for the localization, 2) left ventricular 2-chamber TrueFISP cine, 3) 4-chamber TrueFISP cine, 4) 4 sets of contiguous short-axis TrueFISP cine stack of the two ventricles in which the orientation of each short-axis stack varies (Fig. 1). The short-axis stacks were obtained by aligning the imaging plane parallel to both right and left atrioventricular junctions with one slice cutting through both atrioventricular junctions (*AV Junctions* protocol), aligning the imaging plane parallel to the left AV junction only (*Left AV Junctions* protocol), aligning the plane perpendicular to the septum with one slice acquired through the septal junction (*Septum* protocol) and aligning the imaging plane perpendicular to the long axis of the LV with one slice cutting through the septal junction (*Long Axis* protocol). The contiguous short-axis TrueFISP cine stack parameters were as follows: TR = 45.15 ms, TE = 1.37 ms, slice thickness = 8 mm, FOV = 300 × 300 mm, matrix = 192 × 192, flip angle = 55, parallel imaging factor = 3 and inter-slice gap = 25%, as per SCMR latest acquisition guidelines. The four sequences were acquired in the following order: *Septum, Left AV Junctions, AV Junctions* and *Long Axis*.

### 2.3. CMR image analysis

The segmentation of both the RV and LV was performed on Segment, Medviso software version 3949 [17] which has been 510 k FDA approved.

For LV function assessment, epicardial and endocardial borders were automatically contoured and calculated by selecting the basal and apical short-axis slices. Basal slice was defined as the slice with more than 50% myocardium around the blood during diastole (Fig. 2) as described by the SCMR analysis guidelines [11]. Apical slice was selected as the last slice of the stack with visible ventricular cavity. Manual adjustment of the contours was performed if required. Papillary muscles were estimated and excluded from the LV volume calculation. The adjustment for systolic atrioventricular ring descent was performed automatically by the software with manual selection of the basal descent. The basal descent was estimated by identifying the basal plane at end-systole (ES) and end-diastole (ED) with the inclusion of the slice thickness and inter-slice gap. (Fig. 3). From the delineated contours, the end-diastolic volume (EDV) and end-systolic volume (ESV) were computed using the summation of disc method. Both stroke volume (SV) and ejection fraction (EF) were determined for LV function assessment. SV was computed by subtracting the ESV from EDV while EF was determined by dividing the SV by the EDV.

Endocardial borders were manually contoured at end-systole and end-diastole for RV function assessment from the most basal to the most apical slices. RV end-systolic and end-diastolic frames were selected based on LV end-systolic and end-diastolic frames which were determined by the software after LV segmentation. RV basal slice was defined as the first RV slice not superior to the level of the tricuspid valve (Fig. 4) [11]. Trabeculations and papillary muscles were included in the determination of the RV volumes. Similar

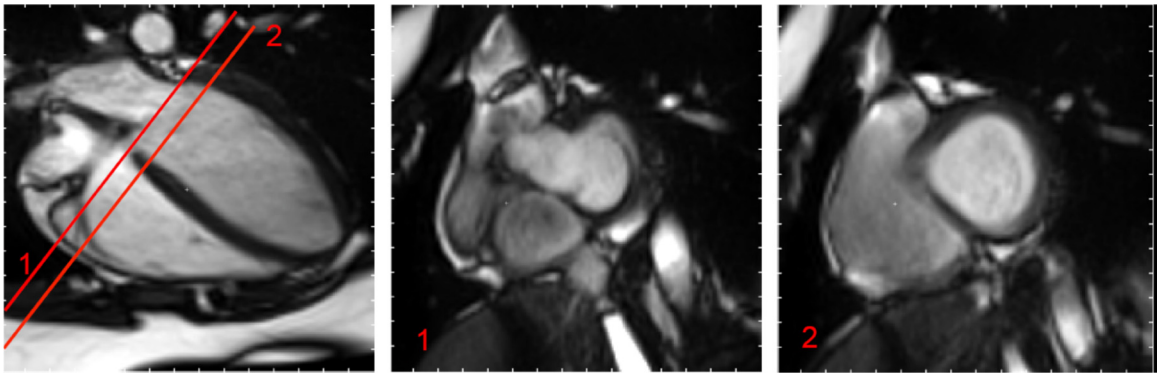


**Fig. 2.** Basal short-axis slice selection for the left ventricle. Illustration of the basal plane selection following the SCMR guidelines [11]. "The left atrium can be identified when less than 50% of the blood volume is surrounded by myocardium and the blood volume cavity is seen to be expanding during systole". The basal slice is the slice with more than 50% of myocardium muscle around the blood. In this example, slice 1 is in the left atria while slice 2 is the ventricle and can therefore be considered as the basal slice.

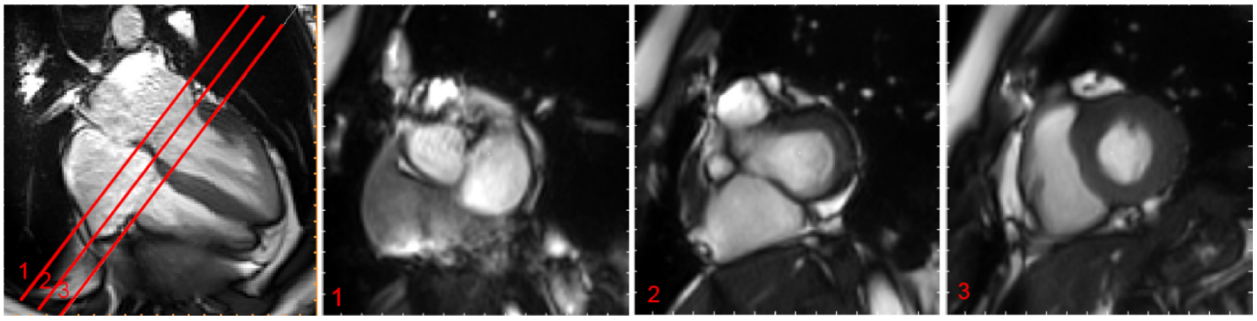


**Fig. 3.** Basal descent selection for the left ventricle. Example of the basal descent estimation following the SCMR guidelines [11]. Using cross-referencing from long axis locations and the definition of the basal plane, we estimate the basal plane at end-systole to be between slice 2 and slice 3 when the basal plane at end-diastole was slice 1. We therefore estimate the basal descent to be 1.5× resolution in z, in our case (8 mm thickness and 25% gap) this gives 15 mm.


**Fig. 4.** Basal short-axis slice selection for the right ventricle. Illustration of the basal plane selection following SCMR guidelines [11]: RV basal slice was defined as the first RV slice not superior to the level of the tricuspid valve. In this example, slice 1 is superior to the level of tricuspid valve while slice 2 is the first slice not superior to the level of the tricuspid valve and thus it is considered as the basal slice.

to LV volumes determination, SV and EF were computed from the delineated RV endocardial contours. The RV and LV stroke volumes obtained should be similar when no intra-or extra-cardiac shunts are present [11]. LV stroke volume was then used to cross-reference with the RV stroke volume as the determination of the LV volume data is considered more reliable compared to the determination of the RV volume data.

RV mass estimation is not defined by the SCMR guidelines as part of a standard cardiac function evaluation so the RV epicardium was not delineated. For a fair comparison between LV and RV, the LV mass was not included in this study.

### 2.4. Reproducibility

With the absence of known truth, assessing the variability between observers and observations is considered the optimal method to evaluate the accuracy of a method. Inter and intra-observer reproducibility was estimated in this study on the 80 cine sequences (20 subjects with 4 sequences). First, the sequences were analysed by 2 trained analysts following the SCMR guidelines as described previously. The first observer analysed all 80 sequences a second time after 2 months to assess intra-observer reproducibility. Eight parameters were recorded from the LV and RV endocardium delineations: EF, SV, the basal slice position at ED and the basal slice position at ES. In addition, since the complete protocol could not be retested to assess acquisition reproducibility, all sequences

were verified by a radiographer and a mark of 1 was given for every sequence that follow the prescribed protocol, 0 otherwise.

### 2.5. Statistical analysis

Statistical analysis was performed using Matlab version R2013b. For each acquisition protocol, the segmentation results from the 2 observers were compared following Bland–Altman method [18] (available Matlab code from [19]) and the coefficients of variation (CV) recorded. Lin's concordance correlation coefficient (CCC) [20] was used to further assess the agreement between two observers. Lin's CCC varies from 0 to 1 where 1 represents perfect agreement. The same analysis was performed between the two sets of observations from the same observer. Finally, the mean value (and standard deviation) of the EF and SV across the 20 subjects was calculated for each protocol to determine the influence of the short-axis plane on the measurements themselves and pair-wise Bland Altman analysis and Pearson correlation was used to differentiate the protocols.

## 3. Results

Data was successfully acquired for all 20 volunteers and the image quality considered sufficient for the analysis. Therefore all 80 sequences were included in the statistical analysis.

### 3.1. Image acquisition

The 80 short axis sequences were evaluated in order to measure the accuracy of the acquisition protocol. The *Septum* protocol reached the highest accuracy score with 18/20 correct planning, while the *AV Junctions* reached 15/20, the *Long Axis* reached 13/20 and the *Left AV Junctions* was the hardest to plan with a score of 12/20. Given the risk of patient movement (and breath-hold positioning related differences) between scans, one could expect that the acquisition reproducibility would depend on the order at which the protocols were planned due to the time delay with the planning view. However, the least reproducible protocol (*Left AV Junctions*) was the second one to be planned.

### 3.2. Image analysis

Each sequence required a fair amount of manual correction for the LV after using the automatic algorithm provided by the software. This mainly consisted in detecting and delineating the basal and apical slices. Each sequence required 10 min on average for LV segmentation and another 10 min for RV segmentation. No differences in terms of manual corrections or processing time were noticed.

The principal observed difference in the 4 short-axis orientations is the choice of the basal slice to include in the segmentation. Fig. 5 gives an example for one subject in which the four definitions of the short-axis orientation led to 4 distinctly different planes. In this case, right ventricular basal slice was different from the left ventricular basal slice for 2 out of 4 protocols. This dispersion would be different at end-systole since the heart contracts radially, vertically and circumferentially.

### 3.3. Inter-observer reproducibility of the protocols

Table 1 displays the Bland–Altman CV and Lin's CCC for each 4 protocols. Variability for the RV is significantly higher (p-value < 0.05) than the LV variability for every protocol (mean EF CV = 4.81% for the LV, mean EF CV = 9.17% for the RV).

The *AV Junctions* protocol reaches the highest inter-observer reproducibility for the LV clinical parameters (CV = 4.20%, CCC = 0.86 for EF and CV = 5.67%, CCC = 0.97 for SV) as well as the RV SV (CV = 9.08%, CCC = 0.91) but the lowest reproducibility for the RV EF (CV = 11.08%, CCC = 0.40), correlated with the lowest reproducibility for the choice of the basal slice at ED and ES. The *Septum* protocol has the second highest LV measurement reproducibility (EF CCC = 0.82, CV = 4.61%). In addition, the variability of the measures for the RV using the *Septum* protocol is the lowest (CV = 7.62% and CCC = 0.69 for the EF) with a higher reproducible choice of the basal slices. Finally, the *Left AV Junctions* and the *Long Axis* protocol show similar behavior, giving performances slightly poorer than previously discussed protocols for the LV, in the middle range for the RV. Fig. 6 presents the Bland Altman and correlation plots of the *Septum* and *AV Junctions* protocols for the LV and RV EF. For both acquisition protocols similar results for the LV are obtained but variability is significantly reduced using the *Septum* orientation for the RV.

**Table 1**
Inter-observer reproducibility parameters. CV: coefficient of variation, CCC: Lin's concordance correlation coefficient.

| | | Left Ventricle | | Right Ventricle | |
|---|---|---|---|---|---|
| | | CV | CCC | CV | CCC |
| AV Junctions | EF | **4.20** | **0.86** | 11.08 | 0.40 |
| | SV | 5.67 | **0.97** | **9.08** | **0.91** |
| | Basal ED | 10.64 | 0.92 | 16.45 | 0.73 |
| | Basal ES | 4.95 | 0.96 | 16.50 | 0.32 |
| Left AVJunctions | EF | 5.24 | 0.78 | 9.54 | 0.59 |
| | SV | 9.17 | 0.92 | 15.53 | 0.79 |
| | Basal ED | 11.00 | 0.93 | 16.74 | 0.87 |
| | Basal ES | 7.05 | 0.94 | 10.52 | 0.78 |
| Septum | EF | 4.61 | 0.82 | **7.62** | **0.69** |
| | SV | **5.55** | 0.96 | 12.02 | 0.87 |
| | Basal ED | 15.42 | 0.89 | 14.45 | 0.88 |
| | Basal ES | 9.52 | 0.92 | 9.17 | 0.87 |
| Long Axis | EF | 5.20 | 0.76 | 8.42 | 0.56 |
| | SV | 7.49 | 0.94 | 11.40 | 0.89 |
| | Basal ED | 10.47 | 0.93 | 12.47 | 0.90 |
| | Basal ES | 7.20 | 0.92 | 8.55 | 0.88 |

**Table 2**
Intra-observer reproducibility parameters. CV: coefficient of variation, CCC: Lin's concordance correlation coefficient.

| | | Left Ventricle | | Right Ventricle | |
|---|---|---|---|---|---|
| | | CV | CCC | CV | CCC |
| AV Junctions | EF | 3.85 | 0.88 | **6.47** | **0.70** |
| | SV | **4.20** | **0.98** | **8.01** | 0.91 |
| | Basal ED | 0.00 | 1.00 | 21.41 | 0.73 |
| | Basal ES | 5.80 | 0.94 | 10.69 | 0.76 |
| Left AVJunctions | EF | 4.61 | 0.84 | 8.70 | 0.58 |
| | SV | 6.26 | 0.96 | 9.35 | **0.93** |
| | Basal ED | 7.52 | 0.97 | 15.59 | 0.90 |
| | Basal ES | 5.77 | 0.95 | 10.73 | 0.76 |
| Septum | EF | 3.62 | 0.86 | 8.25 | **0.70** |
| | SV | 5.22 | 0.97 | 9.39 | **0.93** |
| | Basal ED | 18.42 | 0.82 | 13.24 | 0.93 |
| | Basal ES | 12.61 | 0.82 | 8.00 | 0.89 |
| Long Axis | EF | **3.25** | **0.91** | 7.93 | 0.61 |
| | SV | 4.70 | 0.98 | 8.93 | 0.92 |
| | Basal ED | 7.16 | 0.96 | 11.92 | 0.92 |
| | Basal ES | 4.56 | 0.97 | 7.01 | 0.92 |

### 3.4. Intra-observer reproducibility of the protocols

Table 2 presents the intra-observer reproducibility results for each short-axis acquisition plane, in the same format as Table 3. As one would expect, global intra-observer reproducibility is higher than inter-observer reproducibility. This is true for both ventricles

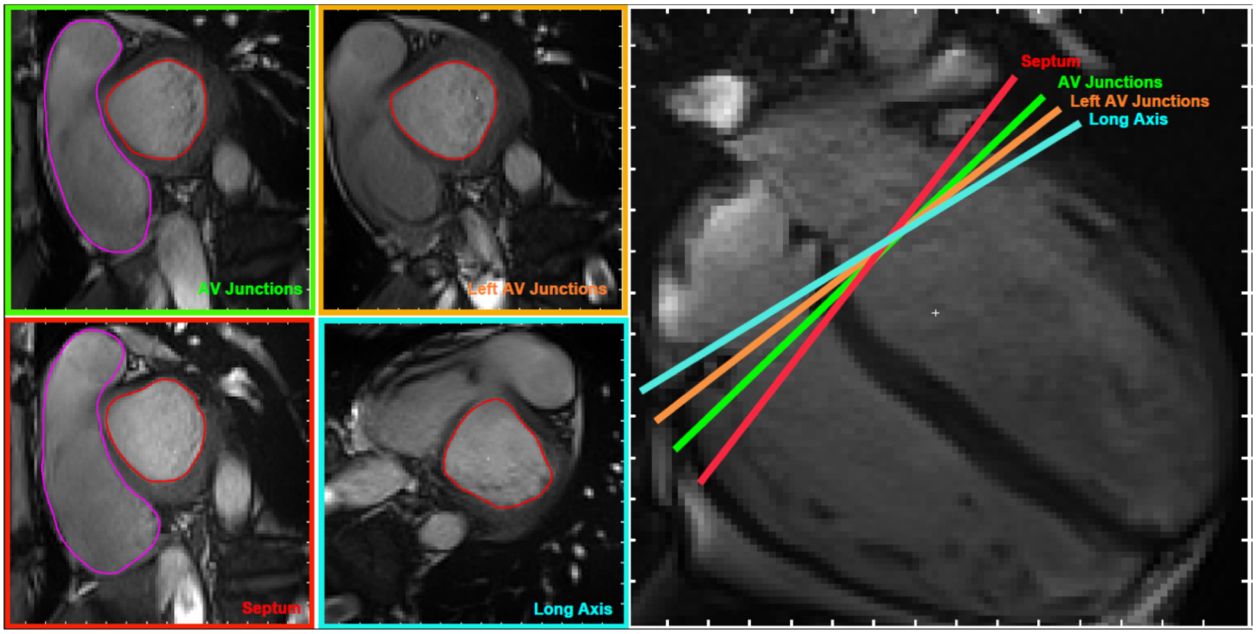


**Fig. 5.** Example of basal slice selection for the four acquisition planes. (Left) Example of selected basal slice at end-diastole for the four protocols. (Right) Slice positions on the 4-chamber view. In this example, the 4 definitions led to 4 distinct basal slices. This impacts the segmentation for both the right and left ventricles.

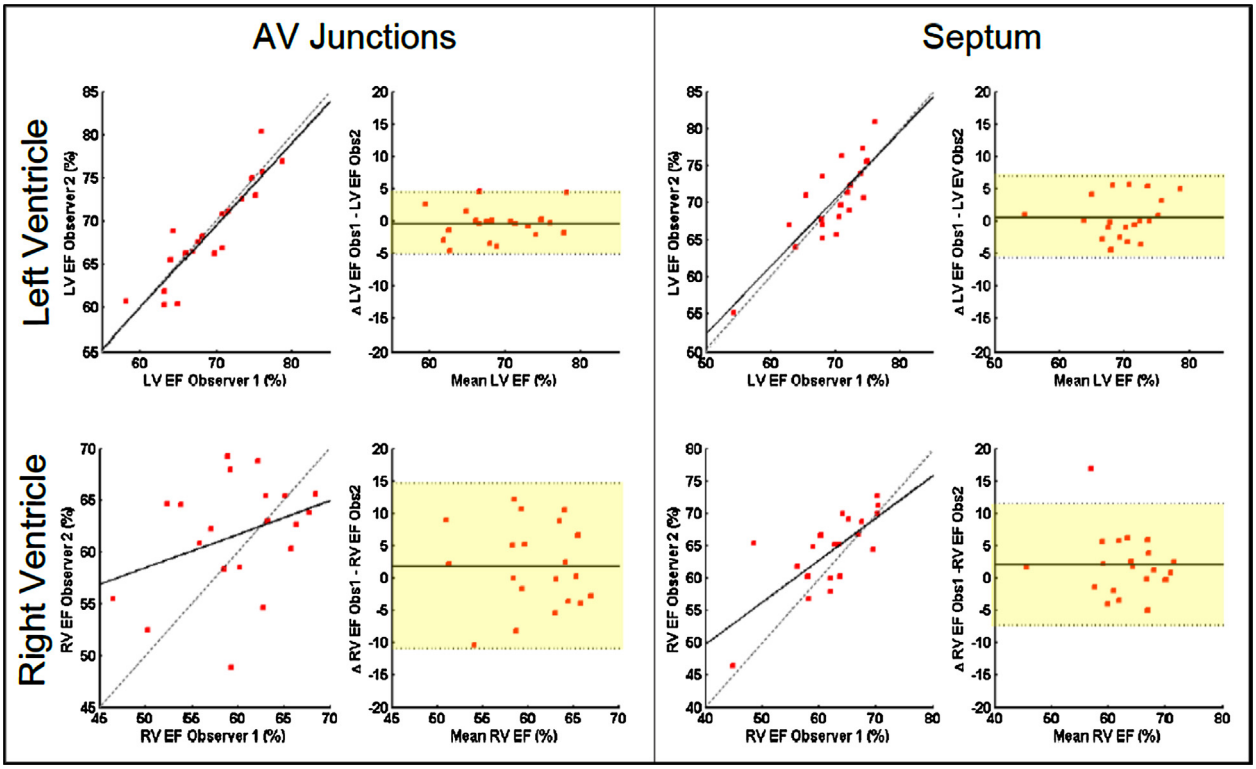


**Fig. 6.** Bland-Altman plots: inter-observer reproducibility of the *Septum* and *AV Junctions* protocols. Comparison of two protocols in terms of reproducibility for the left and right ejection fraction.

**Table 3**
Parametric comparison of the four protocols. CV: coefficient of variation, $R^2$: Pearson's correlation coefficient.

| | AV junctions | | Left AV junctions | | Septum | | Long axis | | CV | | $R^2$ | |
|---|---|---|---|---|---|---|---|---|---|---|---|---|
| | Mean | Std | Mean | Std | Mean | Std | Mean | Std | Mean | Std | Mean | Std |
| LV EF (%) | 68.81 | 5.39 | 68.94 | 5.10 | 69.36 | 5.00 | 68.64 | 4.58 | 4.35 | 0.48 | 0.85 | 0.04 |
| LV SV (ml) | 92.90 | 20.27 | 95.51 | 21.78 | 95.13 | 21.07 | 93.43 | 21.05 | 7.02 | 0.46 | 0.94 | 0.02 |
| RV EF (%) | 60.05 | 5.02 | 59.82 | 5.64 | 61.08 | 6.22 | 61.03 | 4.85 | 9.95 | 1.23 | 0.52 | 0.10 |
| RV SV (ml) | 92.20 | 20.39 | 95.16 | 22.79 | 94.50 | 21.19 | 94.82 | 20.60 | 10.02 | 0.95 | 0.90 | 0.03 |

where the mean CV for the EF is 3.8% for LV and 7.8% for RV compared respectively to 4.8% and 9.1% for inter-variability. For the LV, all 4 protocols give similar levels of reproducibility for both the EF and SV, including the *Septum* protocol which shows less reproducibility in the choice of the basal slices. For the RV, the *AV Junctions* method gives the highest CV for the SV and EF but the *Septum* protocol shows the larger Lin's CCC.

### 3.5. Parametric influence of the protocols

No significant difference was observed for the measurements of the LV and RV EF and SV between the protocols when averaged over all the subjects. Table 3 presents the means and standard deviations of the cited parameters for each of the 4 acquisition methods. In addition, the average Bland Altman CV and Pearson coefficient over the 6 pairs of protocols are given. The Left SV and Right SV are highly similar independently of the protocol, which is expected for healthy volunteers. The mean values of the parameters are extremely similar for all protocols. However, the CV is important (9.95%, larger than the reproducibility CV) for the RV and the correlation not satisfying ($R^2 = 0.52 \pm 0.1$) for the EF.

## 4. Discussion

Globally, reproducibility results demonstrated in this study are in agreement with values reported in the literature for both the left (CV = 5.4% in [10]) and the right ventricle (CV = 8.9% for short-axis in [12]). This tends to confirm the observers' expertise in this study as well as the image quality representative of clinical studies. No significant differences were found in the intra or inter variability between protocols for the LV measurement, despite a slight improvement of the reproducibility when using the *AV Junctions* plane. Additionally, the 4 studied protocols led to similar mean values of the clinical parameters for both LV and RV. This suggests that for studies between groups of population, the acquisition protocol will not influence the results. These results confirm CMR ability to give robust and reproducible evaluation of the LV using current practice. Clinically acceptable reproducibility of LV assessment is reached thanks to exiting analysis guidelines [11] and despite the lack of details on the short-axis plane in the acquisition guidelines [13,14].

However, the high coefficient of variation between protocols for the measurement of RV EF, higher than the intra and inter variability, suggests that reliable comparison between subjects can only be reached using the same protocol, at least for the RV. Indeed, RV evaluation still remains a challenge using CMR due to the complex shape of the ventricle, its thinness, the trabeculations and the blood motion especially toward the basal area where the ventricle splits into the right atrium and the pulmonary artery. All these features make precise delineation of the RV endocardium and the selection of its boundaries prone to high observer-variability. Current SCMR guidelines for RV assessment are limited due to the difficulty of setting a general rule and therefore the basal slice detection is based on cross-referencing with the long axis view, where the tricuspid valve can better be seen. The present study demonstrates that despite current SCMR RV assessment guidelines, observer-variability is high; therefore, improvement should be considered in the acquisition protocol instead of the analysis protocol.

Previous studies on optimal acquisition protocol for increased robustness of RV evaluation have already been conducted [12,15]. While Alfakih et al. [12] have recommended long-axis cine acquisition, Strugnell et al. [15] used a set of multi-slice images in a plane perpendicular to a line from the center of the pulmonary valve to the apex of the RV in order to see the tricuspid valve on the modified short-axis slices. For RV only studies, these recommendations can be followed since the level of variability is lower than the presented results. However, these acquisition protocols are sub-optimal or not applicable for LV assessment.

Many studies require both ventricles to be evaluated simultaneously in order, for instance, to measure the regurgitant volume, evaluate dyssynchronous motion or confirm the presence of septal shift. Furthermore, according to Friedberg and Redington [21], LV and RV should not be considered as separate entities since their interactions are also the cause of cardiac failures. Therefore, although long-axis acquisitions seem to decrease observer-variability due to the limit of the right ventricle best viewed on the long-axis plane, in clinical practice the cine acquisition protocol would have to be significantly extended if both ventricles needed to be evaluated separately. CMR acquisition usually also includes other imaging sequences to characterize the flow, perfusion or the structure of the heart, leading to a protracted scanning times. Thus, additional imaging may not be the best approach. In this study, we suggested to standardize the current protocol by defining an optimal short-axis plane that would increase RV assessment accuracy without decreasing LV assessment accuracy for LV-RV function evaluation. We found that the *Septum* protocol was significantly better than the other 3 protocols for the RV measurement, enabling an inter-variability acceptable in clinical practice.

This study suffers some limitations. First, there exists no ground truth to validate the presented results to ensure the consistency of the analysis. This is why this study relies on reproducibility. The study was monocentric and involved only healthy volunteers, not representative of diseased patients that undergo CMR imaging. The same study could not be performed on patients due to the lengthy protocol (40 min instead of the standard 10 min). However, the volunteers were multicultural, multinational with various body weight and size to increase variability in the heart geometry. Moreover, we have shown that the most robust protocol to plan was the *Septum* protocol. This is due to the septal muscle being the most visible feature in the long-axis view, as it is thicker and more stable than the junctions, whether or not the heart is healthy. We therefore believe that the influence of each protocol on the reproducibility would still be valid in a diseased population.

## 5. Conclusion

To conclude, for LV only studies, the chosen short-axis acquisition plane has no significant influence but the *AV Junctions* plane would be preferred as it led to more inter and intra-observer reproducible results and has proved to be robust in the planning. For RV only studies, none of the tested short-axis protocols could reach the level of reproducibility reported for the axial plane. Therefore, an axial plane should be preferred. Finally, when both ventricles are studied simultaneously, which would be recommended for most clinical trials or diagnostic scans, the *Septum* protocol gives the highest reproducibility results for the RV while maintaining the LV reproducibility to a high level. In addition, the *Septum* protocol has the added advantage of being the easiest to plan. Based on these results, the authors would recommend to acquire the *Septum* protocol (short-axis slices are perpendicular to the septum with one cutting through the septum junction) when both ventricles are studied and a single technique is adopted.

## Conflict of interest

The authors declare no conflict of interest.

## Acknowledgment

This work has been partially funded by the NMRC NUHS Centre Grant – Medical Image Analysis Core (NMRC/CG/013/2013).

## References

[1] F. Grothues, G.C. Smith, J.C. Moon, N.G. Bellenger, P. Collins, H.U. Klein, D.J. Pennell, Comparison of interstudy reproducibility of cardiovascular magnetic resonance with two-dimensional echocardiography in normal subjects and in patients with heart failure or left ventricular hypertrophy, Am. J. cardiol. 90 (1) (2002) 29–34.
[2] S.G. Myerson, N.G. Bellenger, D.J. Pennell, Assessment of left ventricular mass by cardiovascular magnetic resonance, Hypertension 39 (3) (2002) 750–755.
[3] N.G. Bellenger, J.M. Francis, C.L. Davies, A.J. Coats, D.J. Pennell, Establishment and performance of a magnetic resonance cardiac function clinic, J. Cardiovasc. Magn. Reson. 2 (1) (2000) 15–22.
[4] M.G. Danilouchkine, J.J. Westenberg, A. de Roos, J.H. Reiber, B.P. Lelieveldt, Operator induced variability in cardiovascular MR: left ventricular measurements and their reproducibility, J. Cardiovasc. Magn. Reson. 7 (2) (2005) 447–457.
[5] A.K. Attili, A. Schuster, E. Nagel, J.H. Reiber, R.J. van der Geest, Quantification in cardiac MRI: advances in image acquisition and processing, Int. J. Cardiovasc. Imaging 26 (1) (2010) 27–40.
[6] T.D. Karamitsos, L.E. Hudsmith, J.B. Selvanayagam, S. Neubauer, J.M. Francis, Operator induced variability in left ventricular measurements with cardiovascular magnetic resonance is improved after training, J. Cardiovasc. Magn. Reson. 9 (5) (2007) 777–783.
[7] C.F. Mooij, C.J. de Wit, D.A. Graham, A.J. Powell, T. Geva, Reproducibility of MRI measurements of right ventricular size and function in patients with normal and dilated ventricles, J. Magn. Reson. Imaging 28 (1) (2008) 67–73.
[8] P.M. Pattynama, H.J. Lamb, E.A. Van der Velde, R.J. Van der Geest, E.E. Van der Wall, A. De Roos, Reproducibility of MRI-derived measurements of right ventricular volumes and myocardial mass, Magn. Reson. Imaging 13 (1) (1995) 53–63.
[9] F. Grothues, J.C. Moon, N.G. Bellenger, G.S. Smith, H.U. Klein, D.J. Pennell, Interstudy reproducibility of right ventricular volumes, function, and mass with cardiovascular magnetic resonance, Am. Heart J. 147 (2) (2004) 218–223.
[10] J. Caudron, J. Fares, V. Lefebvre, P.-H. Vivier, C. Petitjean, J.-N. Dacher, Cardiac MRI assessment of right ventricular function in acquired heart disease: factors of variability, Acad. Radiol. 19 (8) (2012) 991–1002.
[11] J. Schulz-Menger, D.A. Bluemke, J. Bremerich, et al., Standardized image interpretation and post processing in cardiovascular magnetic resonance: society for cardiovascular magnetic resonance (SCMR) board of trustees task force on standardized post processing, J. Cardiovasc. Magn. Reson. 15 (35) (2013).
[12] K. Alfakih, S. Plein, T. Bloomer, T. Jones, J. Ridgway, M. Sivananthan, Comparison of right ventricular volume measurements between axial and short axis orientation using steady-state free precession magnetic resonance imaging, J. Magn. Reson. Imaging 18 (1) (2003) 25–32.
[13] S. Fratz, T. Chung, G.F. Greil, et al., Guidelines and protocols for cardiovascular magnetic resonance in children and adults with congenital heart disease: SCMR expert consensus group on congenital heart disease, J. Cardiovasc. Magn. Reson. 15 (51) (2013).
[14] C. Kramer, J. Barkhausen, S. Flamm, R. Kim, E. Nagel, Society for cardiovascular magnetic resonance board of trustees task force on standardized protocol. Standardized cardiovascular magnetic resonance imaging (CMR) protocols, society for cardiovascular magnetic resonance: board of trustees task force on standardized protocols, J. Cardiovasc. Magn. Reson. 10 (35) (2008).
[15] W.E. Strugnell, R.E. Slaughter, R.A. Riley, A.J. Trotter, H. Bartlett, Modified RV short axis series-a new method for cardiac MRI measurement of right ventricular volumes, J. Cardiovasc. Magn. Reson. 7 (5) (2005) 769–774.
[16] C.M. Kramer, J. Barkhausen, S.D. Flamm, R.J. Kim, E. Nagel, et al., Standardized cardiovascular magnetic resonance (cmr) protocols 2013 update, J. Cardiovasc. Magn. Reson. 15 (1) (2013) 1.
[17] Heiberg, E. Wigstrom, L. Carlsson, M. Bolger, A. Karlsson, Time resolved three-dimensional automated segmentation of the left ventricle, Comput. Cardiol. (2005) 599–602 (IEEE).
[18] J.M. Bland, D. Altman, Statistical methods for assessing agreement between two methods of clinical measurement, Lancet 327 (8476) (1986) 307–310.
[19] R. Klein, J.M. Renaud, M.C. Ziadi, S.L. Thorn, A. Adler, R.S. Beanlands, et al., Intra-and inter-operator repeatability of myocardial blood flow and myocardial flow reserve measurements using rubidium-82 pet and a highly automated analysis program, J. Nucl. Cardiol. 17 (4) (2010) 600–616.
[20] I. Lawrence, K. Lin, A concordance correlation coefficient to evaluate reproducibility, Biometrics (1989) 255–268.
[21] Mark K. Friedberg, Andrew N. Redington, Challenges and opportunities in pediatric heart failure and transplantation: right versus left ventricular failure: differences, similarities, and interactions, Circulation 129 (2014) 1033–1044.